International Journal of Nanomedicine

Dovepress
open access to scientific and medical research

Open Access Full Text Article

ORIGINAL RESEARCH

Rhamnolipid Micelles Assist Azithromycin in Efficiently Disrupting *Staphylococcus aureus* Biofilms and Impeding Their Re-Formation

Shiyu Lin*, Xiaojuan Li*, Yuning Zhang*, Wei Zhang, Gang Shu, Haohuan Li, Funeng Xu, Juchun Lin, Hualin Fu

Innovative Engineering Research Center of Veterinary Pharmaceutics, Department of Pharmacy, College of Veterinary Medicine, Sichuan Agricultural University, Chengdu, Sichuan, 611130, People's Republic of China

*These authors contributed equally to this work

Correspondence: Hualin Fu, Tel +86 28 82691162, Fax +86 28 82652669, Email fuhl2005@sohu.com

Introduction: Biofilm is highly resistant to antibiotics due to its heterogeneity and is implicated in over 80% of chronic infections; these refractory and relapse-prone infections pose a huge medical burden.

Methods: In this study, rhamnolipid (RHL), a biosurfactant with antibiofilm activity, was loaded with the antibiotic azithromycin (AZI) to construct a stable nanomicelle (AZI@RHL) that promotes *Staphylococcus aureus* (*S. aureus*) biofilm disruption.

Results: AZI@RHL micelles made a destruction in biofilms. The biofilm biomasses were reduced significantly by 48.2% ($P<0.05$), and the main components polysaccharides and proteins were reduced by 47.5% and 36.8%, respectively. These decreases were about 3.1 (15.9%), 7.3 (6.5%), and 1.9 (19.5%) times higher compared with those reported for free AZI. The disruption of biofilm structure was observed under a confocal microscope with fluorescent labeling, and 48.2% of the cells in the biofilm were killed. By contrast, the clearance rates of cells were only 20% and 17% when treated alone with blank micelles or free AZI. Biofilm formation was inhibited up to 92% in the AZI@RHL group due to effects on cell auto-aggregation and eDNA release. The rates for the other groups were significantly lower, with only 27.7% for the RHL group and 12% for the AZI group ($P<0.05$). The low cell survival and great formation inhibition could reduce biofilm recolonization and re-formation.

Conclusion: The antibiofilm efficacy of rhamnolipid was improved through micellar nanoparticle effects when loading azithromycin. AZI@RHL provides a one-step solution that covers biofilm disruption, bacteria inactivation, recolonization avoidance, and biofilm re-formation inhibition.

Keywords: *Staphylococcus aureus*, antibiofilm, rhamnolipid, biosurfactant, nanomicelle

Introduction

Antibiotic abuse has induced an increasing potential for drug resistance, a phenotype of which is bacterial biofilm. Biofilms are implicated in ~65% of microbial infections and over 80% of chronic infections in humans according to the National Institutes of Health (NIH).[1] *Staphylococcus aureus* (*S. aureus*) biofilm can colonize tissues and implantable devices, and generate refractory and relapse-prone infections such as pneumonia, osteomyelitis, and endocarditis. Long-term and multiple antibiotic interventions are advocated in chronic infections, but the diseases end with a poor prognosis because of the biofilm heterogeneity. The dense extracellular polymer (EPS) envelope of biofilms acts as a permeability barrier to small-molecule drugs, although few internalized drugs can also be inactivated by biofilms' enzymes.[2] Worse still, the drug tolerance of embedded cells is 10–1000 times that of bacterioplankton. Antibiofilm strategies involving debridement, bacterial signaling inhibitors, EPS-degrading agents, combinatorial antibiotic therapies, and nanoparticles are being investigated,[3,4] which are mono strategies for early biofilm formation or late biofilm disruption. Strategies should be expected to disrupt the EPS of biofilms directly and kill the exposed bacteria with antimicrobial agents.[5] Thus,

Received: 15 September 2023
Accepted: 21 November 2023
Published: 7 December 2023

Graphical Abstract

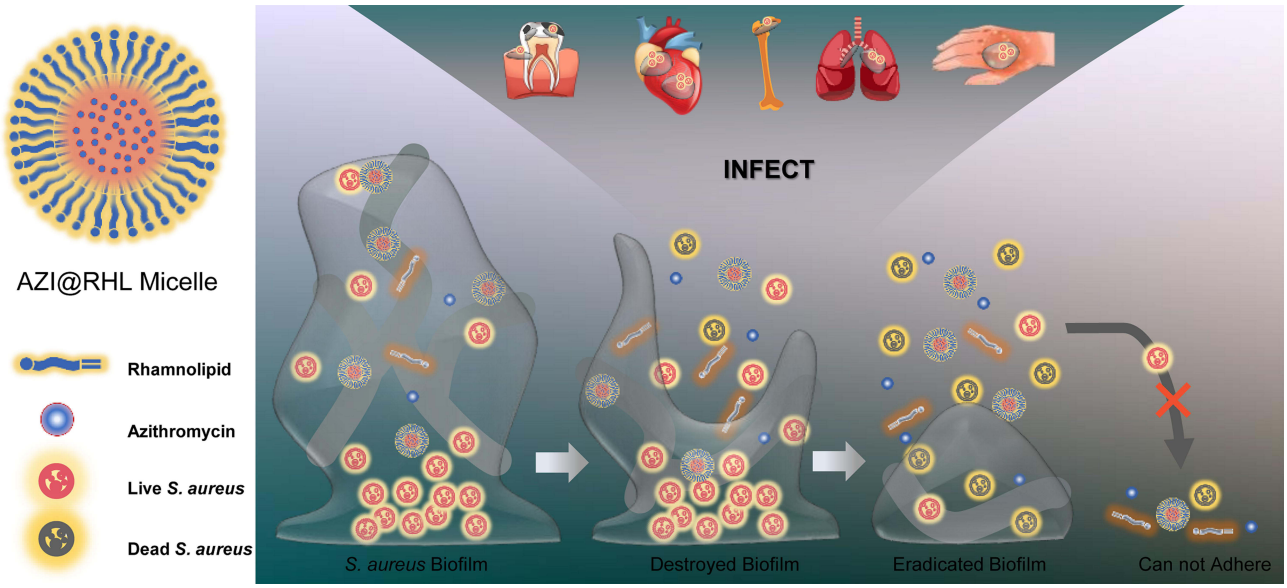

rapid bacteria elimination and biofilm destruction are simultaneously achieved, and the re-adhesion of residual planktonic bacteria should be arrested.

The properties of biosurfactants display potential adjuvant therapeutic agents against bacteria and biofilms.[6,7] Mature biofilms are affected by forming a cavity in their center,[8] and bacterial membranes are deformed due to the biosurfactants inserted into the lipid structure.[9] Cell-to-surface or cell-to-cell interactions can also be altered by their amphipathy, impairing bacteria adhesion and inhibiting biofilm development.[10,11] Rhamnolipids (RHL), a class of metabolites produced by *Pseudomonas aeruginosa* (*P. aeruginosa*), is a recently discovered biosurfactant. Exogenous 0.1% RHL was reported to remove 35% of *S. aureus* biofilms formed on nutrient medium and 86.9% on skim milk medium in only 2 h.[12] They can disrupt biofilms by binding to metal ions within EPS and blocking signaling pathways.[13] RHL can reduce the surface free energy on biofilms and selectively interfere with proteins in EPS.[14] The RHL-involved nanoparticles prepared by Hu et al[15] effectively hindered the adhesion of *helicobacter pylori (H. pylori)* to biotic and abiotic surfaces, removing a critical step in the recurrence of biofilm reinfection. Therefore, RHL can disrupt mature biofilms and inhibit biofilm formation. It also has excellent potential as a carrier box with no toxicity over traditional synthetic surfactants. Amphiphilic RHL self-assembles into micelles when the critical micelle concentration (CMC) is reached. The insoluble drug is encapsulated in its hydrophobic core to increase the drug's solubility.[16] However, RHL is a weak antimicrobial agent due to its fairly large MIC (~2%), so combining it with antibiotics is ideal.[17] Müller et al demonstrated the property of RHL to form stable micelle for the effective loading of hydrophobic drugs, including Nile red, dexamethasone, and tacrolimus, for drug delivery to the skin.[18] This pioneering research opens up a new application of RHL as a drug delivery system.

The nanoparticle drug delivery system is an emerging drug delivery technology with low toxicity, slow release, high efficiency, long-lasting effect, stability, and targeted release.[19,20] Quasi-spherical nanoparticles are highly bactericidal because they induce the production of large-area film stretching and rupture due to their small size, surface effects, quantum size effects, bulk effects, and macroscopic quantum tunneling effects.[21] Nanoparticles with a more remarkable property to act and penetrate biofilm matrices than drug molecules are an emerging strategy for removing mature biofilms.[22] Nanoparticles such as silver, zinc oxide, and nitric oxide interfere with the adhesion of *S. aureus*, thus preventing biofilm formation. The nanoparticles formed by metal integrators and hydrophobic compounds have shown excellent biofilm scavenging activity but are toxicogenic and unsuitable for long-term application.[23]

We hypothesized that the biosurfactant RHL, which disrupts mature biofilms and inhibits biofilm re-formation, can load the azithromycin (AZI) to form stable micelles. The micelles allow the antimicrobial agents to kill bacteria in unison and elevate the antibiofilm efficacy with the nanoparticle effect.

Materials and Methods

Materials

AZI (bulk drug, HPLC≥98%) was purchased from Hubei Zhongmu Anda Co., Ltd (China). RHL was the mixture of mono- and di-rhamnolipid, purchased from Chengdu Ainahua Chemical Preparation Co., Ltd (China). FITC-Con A, MTT, and BCA Protein Assay Kits were from Sigma (USA). LIVE/DEAD BacLightTM Bacterial Viability Detection Kits were from Thermo (USA). Ethanol, acetonitrile, phosphoric acid, dipotassium hydrogen phosphate, monopotassium phosphate, agar powder, crystal violet, sodium acetate, etc., were purchased from Chron Chemicals (China). LB broth and tryptone soybean broth (TSB) were from Hopebio (China).

S. aureus strain (ATCC 25923) was obtained from the Veterinary Drug Safety Assessment Laboratory of Sichuan Agricultural University.

Preparation of Micelles

The critical micelle concentration (CMC) value of the RHL solution was determined by measuring the surface tension values using a Fisher autotensiomat equipped with a DeNuoy ring. We adopted a bottom-up approach for the direct preparation of micelles. AZI and RHL were stirred in methanol for 20 min, and the solution was transferred into a round flask. Methanol was evaporated for 15 min at 60 °C under pressure with RE-2000 rotary evaporators (JinYe, China). Distilled water was added, and the step was continued for 30 min at 60 °C without pressure. The samples were filtered using 0.22 μm filter after cooling down to room temperature. The unencapsulated drugs were removed by ultrafiltration (molecular weight: 10 kd, Merck, USA).

Characterization of Micelles

The nanoparticles' particle size and Z-potential were measured by dynamic light-scattering methods using zetasizer nanoZS90 (Malvern, UK). Nanoparticle samples for transmission electron microscopy (TEM) were stained with 1% phosphotungstic acid and imaged using JEM1400 TEM (JOEL, Japan). For the measurement of the encapsulation efficiency and loading efficiency of AZI in micelles, the samples were disintegrated with methanol and assessed by high performance liquid chromatography (HPLC, Agilent 1100, USA). The in vitro release of AZI@RHL micelles was determined by dialysis bags (D2000, Solarbio, China) in a 100 rpm shaker at 37 °C, with phosphate buffer (pH=7.4) as the release medium. The accumulative release rate of AZI was plotted over time. The samples were run through a C18 stationary phase (Kromasil C18 15 μm column, Sweden), and the mobile phase was a mixture of potassium hydrogen phosphate solution (0.025M, pH=8.2), acetonitrile, and water (30:68:2, v/v/v). AZI@RHL micelles in the vial were placed at 60 °C in the dark for the temperature influence test or light intensity of (4500 ± 500) LX illuminator for the light influence test. The stability of AZI@RHL micelles characterized by encapsulation efficiency was examined at 0, 5, and 10 days (d).

Erythrocyte Compatibility

Fresh rabbit blood (containing anticoagulants) was washed with PBS and centrifuged for erythrocyte. In brief, 2% erythrocytes were suspended with PBS for standby. Meanwhile, 0, 8, 16, 32, and 64 μg/mL AZI@RHL micelles were added an equal amount of 2% erythrocyte suspension and incubated at 37 °C for 2 h. Distilled water was used for the positive control group, and PBS was applied for the negative control group. The absorbance of the supernatant was measured at 540 nm by a microplate reader, and the hemolysis rate (%) was calculated according to the following formula.

$$\text{Hemolysisrate}(\%) = \frac{\text{OD}(\text{samples}) - \text{OD}(\text{negativecontrol})}{\text{OD}(\text{positivecontrol}) - \text{OD}(\text{negativecontrol})} \times 100\%$$

Minimal Inhibitory Concentration (MIC)

MIC was determined by standard microtiter broth dilution method as described by Cole et al[21] with modifications.[22] *S. aureus* strains were cultured overnight in TSB at 37 °C and diluted to 1.5×10^6 CFU/mL for standby. In brief, 100 μL of bacteria sample was inoculated in 96-well plates (tissue culture-treated polystyrene; Costar 3595, Corning, USA) with different concentrations of AZI@RHL micelles, drug AZI, or blank RHL micelles (0, 2, 4, 8, 16, 32, and 64 μg/mL) for co-incubation at 37 °C for 12 h. Absorbance was measured with a multifunction reader (Varioskan LUX, Thermo, USA) at 600 nm.

Establishment of the Biofilm-Growth Curve

A biofilm growth curve was needed to illustrate the growth law of biofilms. In brief, 500 μL of *S. aureus* was incubated in 48-well plates at 37 °C for 5 d. All plates were replaced with fresh medium, and one of the plates was treated and quantified every other day. The biofilms were subjected to crystal violet assay. After the planktonic bacteria in the wells were washed out, the biofilms were subjected to a series of processes, namely, fixing with 500 μL of methanol for 15 min, dyeing with 1% crystal violet for 10 min, and decoloring with 33% acetic acid for 10 min. Absorbance was measured at 570 nm.

Disruption of Mature Biofilms

The disruption effect of AZI@RHL micelles on the mature biofilms of *S. aureus* was evaluated. The effect on biofilm biomass was examined by crystal violet and fluorescence staining.[24] According to the growth law, the mature biofilms were formed in an incubator for 3 d and co-incubated with different AZI@RHL micelles, drug AZI, or RHL blank micelles (2, 4, 8, and 16 μg/mL) for 12 h. Safe doses of non-hemolysis were used. The biofilms were then subjected to the crystal violet assay. For fluorescence staining, mature biofilms were cultured in 6-well plates for 3 d and co-incubated with 16 μg/mL AZI@RHL micelles, drug AZI, or RHL blank micelles for 12 h. The biofilms adhered on slides were incubated with 500 μg/mL FITC-Con A in the dark for 30 min and then observed under a confocal laser scanning microscope (CLSM; Leica, Germany) with 488 nm excitation wavelength and 525 nm emission wavelength.

Polysaccharide and Protein Contents in Biofilms

The clearance capacity of AZI@RHL micelles for the polysaccharides and proteins of biofilm matrix constituent was quantitatively determined. Mature biofilms were cultured in 6-well treated plates. The planktonic bacteria were washed off, and the biofilms adhered on slides were eluted with PBS. The supernatant was obtained by centrifuging at 4000 rpm for 10 min. Polysaccharide content was determined by the phenol-sulfuric acid method. In brief, 1 mL of sample was mixed with 0.5 mL of 9% phenol, followed by 5 mL of sulfuric acid. The mixture was then heated in a 100 °C water bath for 15 min. Absorbance was measured at 490 nm. Polysaccharide quantification was carried out using a proper standard curve. Protein content was measured using BCA Assay Kits.

Cell Clearance

The clearance of cells in biofilms was evaluated with Live/Dead Bacterial Viability Detection Kits and observed under a BX53 fluorescence microscope (Olympus, Japan). Mature biofilms were cultured and treated in 6-well plates. The scavenging capacity of AZI@RHL micelles for the cells in biofilms was quantitatively determined by MTT colorimetric assay. In brief, 100 μL of PBS containing 0.5 mg/mL MTT was added and incubated for 4 h. After the liquid was discarded, 200 μL of DMSO was used to dissolve the formazan. Absorbance was measured at 570 nm.

Biofilms Formation

Bacteria were incubated with AZI@RHL micelles, drug AZI, or RHL blank micelles (0, 4, and 8 μg/mL) in 48-well plates at 37 °C for 12 h to evaluate the inhibition effect on the formation of *S. aureus* biofilms. Sub-MIC doses were used. The biofilms were treated as previously mentioned, and absorbance was measured to calculate the inhibition rate.

Initial Adhesion

The inhibition effect of AZI@RHL micelles on the initial adhesion of *S. aureus* was detected by the plate method. *S. aureus* was incubated with 8 μg/mL AZI@RHL micelles at 37 °C for 2 h. Bacteria in the biofilms were resuspended with PBS, then spread on agar plates, and incubated at 37 °C overnight for colony counting.

Auto-Aggregation Capacity

The auto-aggregation capacity of *S. aureus* was detected by the sedimentation method. *S. aureus* specimens were resuspended in PBS and then incubated with 8 μg/mL AZI@RHL micelles at 37 °C for 12 h. Absorbance at 0 and 12 h was measured at 600 nm. Autoaggregation capacity was calculated as (%) = $(A_0–A_{12})/A_0 \times 100\%$.

eDNA Content

S. aureus biofilms were cultured in 6-well plates. Sterile slides were placed in the wells beforehand, and *S. aureus* was incubated with 8 μg/mL AZI@RHL micelles at 37 °C for 12 h. The planktonic bacteria were washed, and the biofilms adhered on slides were eluted with PBS. The elution was centrifuged at 4000 r for 10 min. For eDNA purification, the mixture of 450 μL of sample, 50 μL of 3M sodium acetate, and 1 mL of ethanol was stored at –70 °C for 2 h. Precipitates were obtained by centrifuging at 12,000 rpm for 10 min at 4 °C and were washed with 1 mL of 70% ethanol. eDNA was dissolved with 20 μL of TE buffer finally, and its concentration was measured with a nanodrop ultramicro spectrophotometer (Thermo, USA).

Statistical Analysis

All data were expressed as Mean ± Standard Deviation (S.D.). The statistical software package, SPSS version 19, was used for statistical analysis. Data were analyzed by ANOVA, followed by a post hoc LSD test. Graphs were finished by utilizing GraphPad Prism 6. Statistical significance was accepted at $P < 0.05$.

Results and Discussion

Preparation and Characterization of AZI@RHL Micelles

The novel surfactant-loaded AZI@RHL micelles were fabricated with a bottom-up approach. The exclusive RHL encapsulated the sensitive antibiotic AZI to eradicate *S. aureus* biofilm and inhibit its re-formation. AZI@RHL micelles possessed an average size of 136.3±68.5 nm and an average Z-potential of –23.1±6.8 mV with a good size distribution (Figure 1A and D). Blank micelles without loading AZI have an average size of 150.9±113.0 nm and an average Z-potential of –37.6±4.7 mV (Figure 1A). Decreased particle size of AZI@RHL micelles may be caused by the increased charge repulsion from AZI that favors demicellization.[25] The changes in size and zeta potential confirmed the success of encapsulating AZI in the core of RHL. From the TEM image (Figure 1C), spherical and dispersed micelles are formed and substances were encapsulated in cores. The ideal size of AZI@RHL ensured its subsequent diffusion in the mucus-like biofilm; the particle size is highly correlated with steric hindrance, and the water channels of biofilms allow the passage of particles of about 200 nm.[10] In addition, AZI@RHL micelles had a high encapsulation rate (80.34%) and loading efficiency (19.42%), which significantly increased the solubility of AZI. The cumulative release rate of AZI@RHL was about 29.9% in the first 2 h, and it reached 68.7% at 36 h, indicating that AZI@RHL micelles have a sustained release effect (Figure 1F). The release process fit well with the Ritger-Peppas equation ($Q = 23.7264 (t^{0.2996})$, $R^2=0.9880$), and the release value of 0.2996 indicated that AZI@RHL micelles released AZI mostly through Fick diffusion.[26]

The CMC value of RHL was measured as low as 0.25 mg/mL, which allowed structurally stable nanocarriers. This was consistent with the results of the temperature influence test, where AZI@RHL micelles showed stability at 60 °C (Figure 1G). The property of RHL to withstand high temperatures was also reported.[27] However, AZI@RHL micelles were unstable under intense light for a long time. The freshly prepared micelle solution was brownish-yellow and transparent (Figure 1B). The color gradually lightened up (not shown), accompanied by a significantly decreased encapsulation rate (Figure 1G, $P<0.05$) after intense light exposure. The light-proof storage is necessary, or freeze-

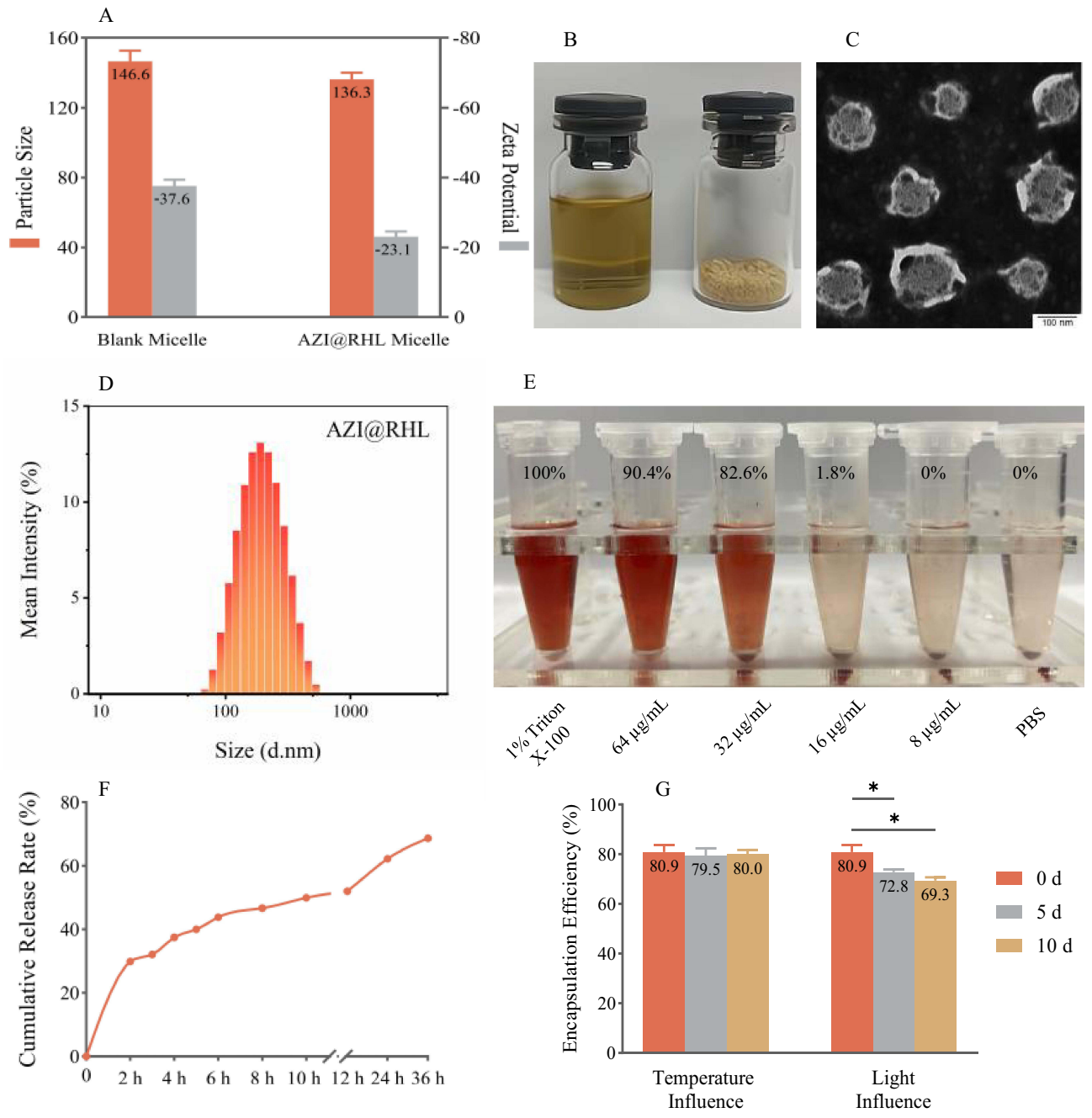

Figure 1 Characterization of AZI@RHL micelles. (**A**) Particle size and zeta potential of blank micelles and AZI@RHL micelles. (**B**) AZI@RHL micelles in different states of solution and lyophilized powder. (**C**) TEM image of AZI@RHL micelles. (**D**) Particle size distribution of AZI@RHL micelles. (**E**) Hemolysis rate (%) of AZI@RHL micelles. 1% triton X-100 was used as the positive control and PBS as the negative control. (**F**) In vitro cumulative release rate of AZI@RHL micelles. (**G**) Encapsulation efficiency of AZI@RHL micelles with the influence of 60 °C and (4500 ± 500) LX. *P<0.05 vs 5 d and 10 d.

drying is also a good option. The lyophilized micelles powder has the characteristics of a faint yellow color, uniform texture, and good reconstitution (Figure 1B). RHL is formed by one or two rhamnoses (hydrophilic) molecules linked to one or two fatty acids (hydrophobic), which are saturated or unsaturated alkyl chains.[28] Intense light accompanied by heat readily oxidizes unsaturated alkyl chains.

The hemocompatibility results (Figure 1E) of AZI@RHL micelles showed that the hemolysis rate was less than 5% at 16 μg/mL, a non-toxic dose range. Meanwhile, 32 μg/mL AZI@RHL resulted in a high hemolysis rate of 82.56%,

suggesting that the dose should be administered via different routes, especially avoiding high intravenous doses. Therefore, our subsequent experimental doses were lower than 16 μg/mL.

Antibacterial Activity

The antibacterial activity of AZI@RHL micelles to planktonic *S. aureus* was investigated by determining the MIC (over 90% inhibition rate) (Figure 2A). All formulations showed different degrees of dose-dependent inhibition. The inhibition rate was 83.14% at 16 μg/mL of AZI and over 90% at 32 μg/mL. Meanwhile, AZI@RHL micelles could inhibit over 90% of bacteria at a concentration of 16 μg/mL. Hence, $MIC_{(AZI)}$ was 32 μg/mL, and $MIC_{(AZI@RHL)}$ was 16 μg/mL. The blank micelles had a weak bacterial inhibition, which is presumed to be one of the reasons for the superior inhibition effect of AZI@RHL micelles over AZI. The production of large area film stretching and rupture induced by nanoparticle surface effects, quantum size effects, bulk effects, and macroscopic quantum tunneling effects may also be a significant reason.[21] This finding demonstrated that the micellar shell has no influence on the interaction of AZI with bacteria.

Establishment of the Biofilm Growth Curve

Prior to biofilm experiments, the growth curve of *S. aureus* biofilm was established (Figure 2B). *S. aureus* biofilm formation is a dynamic process divided into four main stages: 1. Adherence phase: planktonic single cells, self-aggregates, or coaggregates adhered directly to the surface or co-adhered. Most bacteria are still planktonic and are only wrapped in some EPS, which can be reversed. 2. Proliferative phase: activation of specific gene expression induces the massive secretion of EPS and proliferation within the shelter to escape the external attack, which is irreversible. 3. Mature phase: mushroom-like microcolony mature biofilm formed and easily transfer to the next stage due to various factors such as external environment, strain differences, and signaling. 4. Dissemination phase: biofilms are dispersed, and the released bacteria can migrate and reselect new carriers to establish new infections.[2] On the basis of the growth curve of *S. aureus* biofilm, the biofilm formation inhibition experiment should be administered at 0 h with drug treatment of 12 h, and the mature biofilm disruption experiment should be administered after 3 d. The enormity of disrupting mature biofilms and the importance of avoiding recolonization and re-formation could also be seen based on the dynamics and cycling process of the biofilm.

Effect on Mature Biofilm

The biofilm clearance rates were increased in a dose-dependent manner after treated with AZI, blank micelles, and AZI@RHL micelles (Figure 2C). The biofilms showed a maximum clearance of only 15.9% in the presence of AZI. The resistance of *S. aureus* biofilm to AZI was confirmed in previous research.[29] The failure of AZI against biofilms is mainly attributed to the biofilm matrix: the hydrophobic drug fails to penetrate the EPS.[30] Meanwhile, AZI may interact with and be inactivated by the proteins, eDNA, and polysaccharides in EPS.[31] Therefore, antibiotics alone do not provide an excellent antibiofilm effect. RHL exhibited EPS clearance, with 24.7% biofilm clearance of blank RHL micelles at 16 μg/mL. At the same dose, AZI@RHL micelles showed a 48.2% clearance rate of up to 80% at 64 μg/mL (data not shown) and exhibited significant effects over AZI and blank micelles at all doses ($P<0.05$). In addition, AZI@RHL micelles had a clearance rate of 41.8%, which was higher than AZI at their respective sub-MIC. The multifunctional nanoparticle of chitosan/RHL loading clarithromycin (PEG/CLR/RHL_{25} LPNs) prepared by Hu was used to remove *H. pylori* biofilm, and only 59.9% clearance rate of biofilm was achieved with a dose of 160 MIC.[15] The biofilm was further visualized by FITC-Con A specifically labelable binding D-(+)-glucose and D-(+)-mannose moieties of the major component polysaccharides of EPS (Figure 2E). The extensive *S. aureus* biofilm with abundant EPS matrix in the control was observed under a confocal microscope. Consistent with the crystal violet results, the blank micelles showed a slight EPS dispersion effect but almost none was observed for AZI alone. A remarkable reduction in biofilm biomass and thickness was observed after treatment with AZI@RHL micelles. Therefore, RHL could disrupt the critical matrix surrounding the bacteria and assist antibiotics kill the bacteria within biofilms.[32]

The biofilm comprises 10–25% bacterial cells and 75–90% EPS matrix envelope.[33] The effect of AZI@RHL on bacteria and EPS components, including polysaccharides and proteins, was also investigated to further evaluate the antibiofilm activity of AZI@RHL. Mature *S. aureus* biofilms in presence of 16 μg/mL AZI@RHL micelles showed

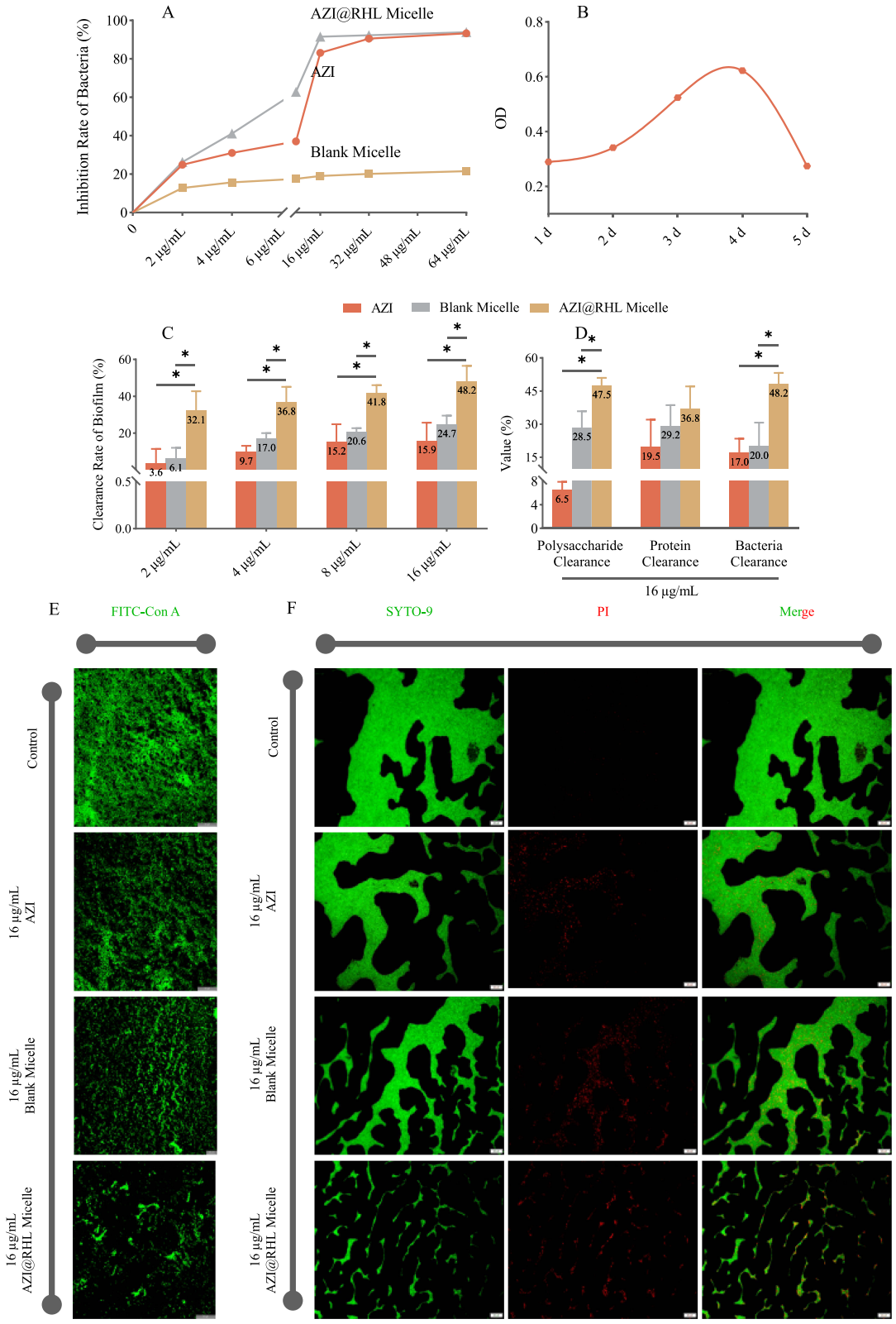

Figure 2 Different effects of AZI, blank micelle, and AZI@RHL micelle on *S. aureus* and mature biofilms. (**A**) Inhibition rate curve of *S. aureus* with different doses of treatment (by AZI). (**B**) *S. aureus* biofilm growth curve for 5 d. Biofilm was quantified through OD value by the crystal violet way. (**C**) Clearance rate of *S. aureus* matures biofilm. **P*<0.05 vs AZI and blank micelle group. (**D**) Clearance rate of polysaccharides, proteins, and bacteria in biofilms. **P*<0.05 vs AZI and blank micelle group. (**E**) Confocal laser scanning micrographs of drug-treated EPS. EPS was visualized by FITC-Con A specifically labelable binding D-(+)-glucose and D-(+)-mannose moieties (Green). The control group was in the absence of drugs. (**F**) Confocal laser scanning micrographs of biofilms and bacteria in them. All cells were labeled green by SYTO-9, and dead ones were labeled red by PI.

significant polysaccharide clearance of 46.79% ($P<0.05$), and the clearance rate of RHL was about half that of AZI@RHL micelle (28.5%). By contrast, the AZI group was less effective at 6.5% polysaccharide clearance rate (Figure 2D). All groups exhibited protein clearance, with AZI, blank micelles, and AZI@RHL micelles reaching the rates of 19.5%, 29.2%, and 36.85%, respectively ($P>0.05$). AZI@RHL micelles caused a more significant reduction in live bacteria, achieving a rate (47.22%) higher than the sum of those for free AZI and RHL blank micelles ($P<0.05$). Almost no difference in bactericidal effect was found between AZI (17.0%) and RHL (20.0%) ($P>0.05$). This result suggested that RHL had a solid property to disrupt *S. aureus* biofilm but not to kill the bacteria, which was consistent with the previous report that RHL could disrupt *Yarrowia lipolytica* biofilm without affecting bacterial growth.[34] Surfactants are often used in sludge dewatering and have the capability of dissolving EPS and converting it to soluble organics.[35] The hydrophilic nature of EPS is mainly due to its components of hydrated polysaccharides, protein, and DNA molecules. Its hydrophobic characteristics are attributed to polysaccharide-linked methyl and acetyl groups. EPS also contains lipids and their derivatives. These biosurfactants can disperse hydrophobic substances in the medium to dissolve EPS.[36] The protein denaturing property of surfactants should be considered.[37] RHL was reported to have the property to disrupt biofilm by mediating signaling pathways, binding metal ions, or some other ways.[38,39]

The biofilm structure and bacteria state inside the biofilm were observed by fluorescence microscopy; all bacteria were labeled green, and the dead ones were labeled red (Figure 2F). The excellent effect of AZI@RHL micelles on the biofilms and bacteria within the biofilms was further confirmed. Numerous green live bacteria within dense biofilms were observed in the control. AZI@RHL micelles showed a good bactericidal property, causing loose biofilm structure, reduced biomass, and many red dead internal bacteria in the merge plot. However, some certain red dead bacteria were observed in all test groups. This finding consistently proved RHL's weak antibacterial activity. Although AZI can harm bacteria by hampering protein synthesis, AZI alone showed no efficacy against embedded bacteria. This phenomenon was attributed to the presence of EPS and to the low antibiotic sensitivity of biofilm bacteria due to reduced growth and inactive metabolism.[40] We speculated that the small size, slightly negative and hydrophilic surface of AZI@RHL micelles allowed the penetration through the EPS and contribute to this result. Therefore, AZI@RHL micelle showed promising results in antimicrobial drug delivery and antibiofilm activity.

Effect on Biofilm Formation

Bacteria dispersed from the impaired biofilm can re-adhere and re-form biofilms on new surfaces, leading to recurrent episodes of infections. In addition to the eradication of mature biofilms, prevention of biofilm re-formation is also essential for the treatment of biofilm-associated infections. After demonstrating the property of AZI@RHL micelle to disrupt biofilms, we verified its inhibitory property. As shown in Figure 3B, AZI@RHL micelles with 1/2MIC (8 μg/mL) and 1/4MIC (4 μg/mL) efficiently inhibited *S. aureus* biofilm formation. AZI@RHL micelles showed 92.13% inhibition at 8 μg/mL, although only 23.74% was achieved at 4 μg/mL ($P<0.05$). Free AZI and blank micelles exhibited poor inhibition, with only 12.0% and 27.7% at 8 μg/mL, respectively, and 6.4% and 14.7% at 4 μg/mL, respectively ($P<0.05$).

The inhibitory property of AZI@RHL micelles on *S. aureus* biofilms was also examined by crystal violet staining. The initial adhesion capacity, auto-aggregation capacity, and eDNA release capacity of *S. aureus* were analyzed to further determine the mechanism. Initial adhesion is the first and critical step in biofilm formation. *S. aureus* can adhere to abiotic surfaces through electrostatic and hydrophobic interactions and biological surfaces by various CWA proteins targeting different substrates. These proteins have different binding specificities for host substrate components such as fibronectin, fibrinogen, and collagen. The hydrophobicity of the bacterial surface is determined by the bacterial surface proteins. After AZI@RHL micelle treatment, the reduced number of colonies on the plate indicated that bacterial adhesion was affected (Figure 3A). RHL is adsorbed on the cell surface and alters the proteins, carbohydrates, and membrane phospholipids on the cell surface through solubilization and the release of apolar membrane components. These alterations probably cause the reduction in cell surface hydrophobicity and the changes in cell permeability or cell lysis, as confirmed by scanning electron microscopy.[41]

After initial attachment, multiple intercellular aggregation factors are produced by *S. aureus* to maintain the stability of the immature biofilm.[3] Cell aggregation is the basis for close contact and signal exchange between bacteria. The rate of bacterial auto-aggregation decreased from 22.3% to 17.1% ($P>0.05$) (Figure 3C) in presence of AZI@RHL micelles.

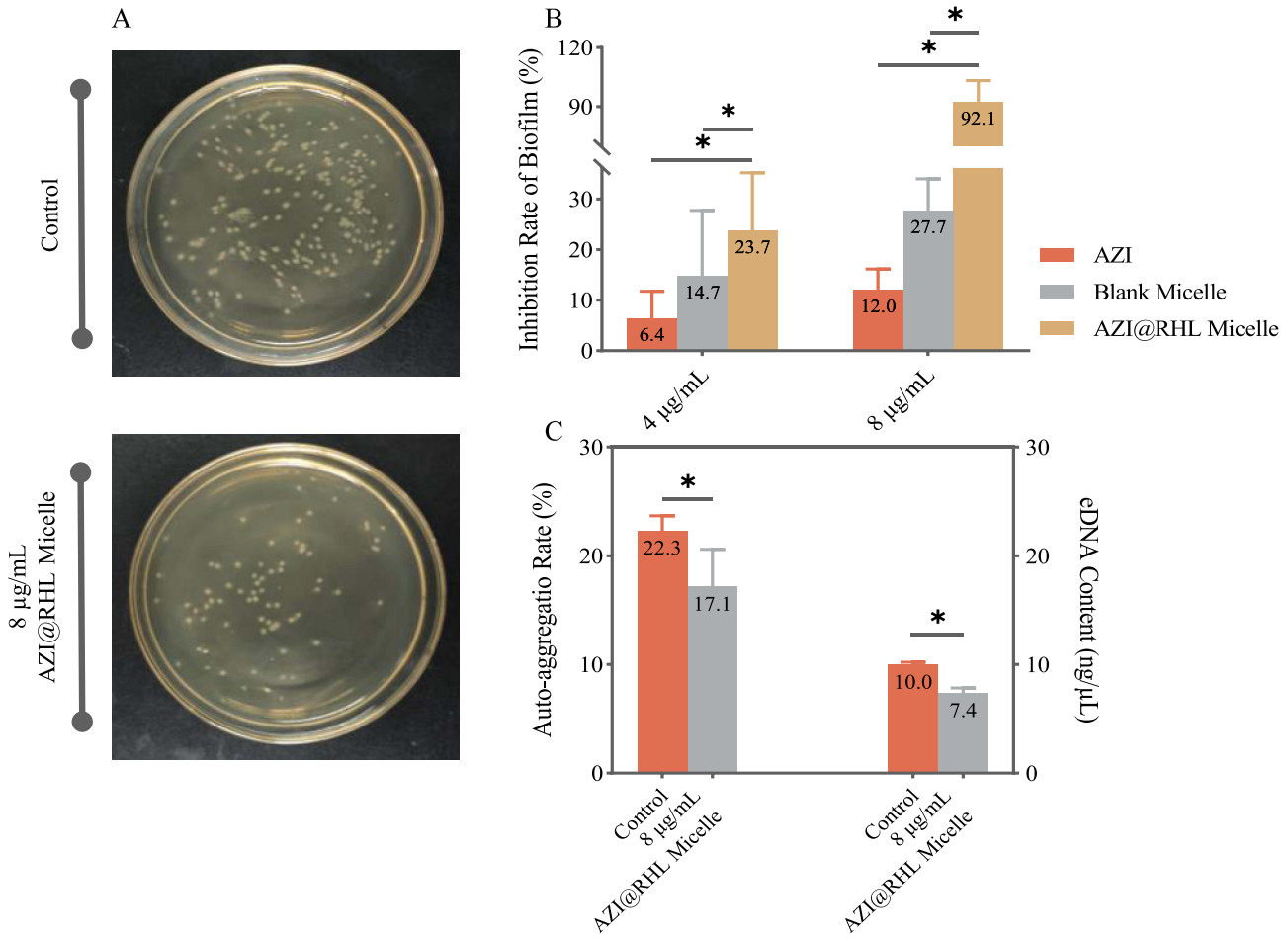

Figure 3 Different effects of AZI, blank micelle, and AZI@RHL micelle on *S. aureus* biofilms formation. (**A**) Effect of 8 μg/mL of AZI@RHL micelles on *S. aureus* initial adhesion. (**B**) Inhibition rate of *S. aureus* biofilm formation after treatment with AZI, blank micelles, and AZI@RHL micelles. **P*<0.05 vs AZI and blank micelle group. (**C**) Auto-aggregation rate of *S. aureus* and the eDNA content in *S. aureus* biofilm formation stage. The control group was in the absence of drugs. **P*<0.05 vs the control group.

Thus, cellular communication was impeded. Surfactants have been considered as additives in biotherapeutic agents owing to their antiaggregation properties.[42] However, marine bacteria aggregation was reportedly assisted by the anionic surfactant, dioctyl sodium sulfosuccinate, at high concentrations.[43] Matrix component eDNA must be released from dead cells into the extracellular environment. eDNA is inserted into transposons or pathogenicity islands of other bacteria and contributes to the communication of virulence factor and antibiotic resistance factor genes. In this study, the amount of eDNA released decreased from 10.0 ng/μL to 7.4 ng/μL, a reduction of 26.09% ($P<0.05$). Cellular communication was further impeded, and biofilm evolution was inhibited. However, whether the low eDNA amount is caused reduced secretion or degradation remains unclear. The key to *S. aureus* biofilm formation is CWA protein-mediated adhesion, information exchange after tight bacterial binding, and substances secretion. The biosurfactant RHL disrupts the bacterial lipid membrane and couples with the micelle-carrying AZI for bacteriostasis, thereby inhibiting biofilm formation.

Overall, the above results demonstrated that AZI@RHL micelles possessed an excellent property to disrupt *S. aureus* biofilm and inhibit its re-formation. However, the effect of AZI@RHL micelles to curb *S. aureus* biofilm infection in vivo needs further research.

Conclusion

Stable AZI-loaded RHL micelles (AZI@RHL) with a high drug-loading efficiency were successfully prepared in a bottom-up approach. RHL can induce the breakdown of bacterial biofilms and affect their structure in their early formation stage and subsequent maturation. Loaded AZI can kill bacteria in the deep biofilm. AZI@RHL showed

enhanced eradicating property to *S. aureus* mature biofilm compared with AZI alone and RHL micelle ghost. It prominently reduced biofilm biomass, eliminated EPS, destroyed biofilm architecture and decreased bacteria viability within the biofilm. Besides, AZI@RHL could also inhibit bacteria adhesion to the abiotic surfaces, auto-aggregation and eDNA release to prevent biofilm regeneration. The results verified that AZI@RHL micelles possessed the most effective antibiofilm activity by combining the disrupting property of RHL and the antibacterial abilities of AZI in a drug delivery system. In summary, AZI@RHL micelles provided a one-step solution to *S. aureus* biofilm problems and highlighted a promising strategy to address persistent *S. aureus* infection. The property of AZI@RHL micelles to counter biofilm infections in vivo must be verified in further trials.

Chemical Compounds Studied in This Article

Azithromycin (PubChem CID: 447043)
Rhamnolipid (PubChem CID: 5458394)
Acetic acid (PubChem CID: 176)
Crystal violet (PubChem CID: 11057)
Methanol (PubChem CID: 887)
PBS (PubChem CID: 24978514)
Agar (PubChem CID: 71571511).

Highlights

- A stable nanomicelle loaded with azithromycin by biosurfactant rhamnolipid was constructed.
- The antibiofilm efficacy of rhamnolipid was improved through micellar nanoparticle effects when loading azithromycin.
- Low cell survival and great formation inhibition could reduce the recolonization and re-formation of biofilms.
- The nanomicelle provides a one-step solution to biofilm problems from disrupting biofilms to impeding their re-formation.

Data Sharing Statement

The source data that support the findings of this study are available on request from the corresponding author.

Ethical Statement

This article does not contain any research involving humans or animals.

Acknowledgments

This work was supported by the College of Veterinary Medicine of Sichuan Agricultural University. We acknowledge the partial support the State Key Laboratory of Crop Gene Exploration and Utilization in Southwest China.

Funding

This research did not receive any specific grant from funding agencies in the public, commercial, or not-for-profit sectors.

Disclosure

The authors declare no competing financial or non-financial interests in this work.

References

1. Lebeaux D, Ghigo JM, Beloin C. Biofilm-related infections: bridging the gap between clinical management and fundamental aspects of recalcitrance toward antibiotics. *Microbiol Mol Biol Rev*. 2014;78(3):510–543. doi:10.1128/MMBR.00013-14
2. Choudhary D, Cassaro CJ. Digging deeper in the biofilm. *Nat Rev Microbiol*. 2021;19(8):484. doi:10.1038/s41579-021-00584-x
3. Schilcher K, Horswill AR. Staphylococcal Biofilm Development: structure, Regulation, and Treatment Strategies. *Microbiol Mol Biol Rev*. 2020;84(3). doi:10.1128/MMBR.00026-19

4. Chen L, Peng M, Zhou J, et al. Supramolecular photothermal cascade nano-reactor enables photothermal effect, cascade reaction, and in situ hydrogelation for biofilm-associated tooth-extraction wound healing. *Adv Mater*. 2023. doi:10.1002/adma.202301664
5. de la Fuente-Nunez C, Reffuveille F, Fernandez L, Hancock RE. Bacterial biofilm development as a multicellular adaptation: antibiotic resistance and new therapeutic strategies. *Curr Opin Microbiol*. 2013;16(5):580–589. doi:10.1016/j.mib.2013.06.013
6. Xiaowen Hu YLYP, Li Y, Piao Y. Two-tailed dynamic covalent amphiphile combats bacterial biofilms. *Adv Mater*. 2023;35(33):e2301623. doi:10.1002/adma.202301623
7. Yizhou Zhan XHYL, Hu X, Li Y. Antimicrobial hybrid amphiphile via dynamic covalent bonds enables bacterial biofilm dispersal and bacteria eradication. *Adv Funct Mater*. 2023;33(23):2214299. doi:10.1002/adfm.202214299
8. Boles BR, Thoendel M, Singh PK. Rhamnolipids mediate detachment of *Pseudomonas aeruginosa* from biofilms. *Mol Microbiol*. 2005;57(5):1210–1223. doi:10.1111/j.1365-2958.2005.04743.x
9. Diaz DRM, Banat IM, Dolman B, Winterburn J, Martin PJ. Sophorolipid biosurfactants: possible uses as antibacterial and antibiofilm agent. *N Biotechnol*. 2015;32(6):720–726. doi:10.1016/j.nbt.2015.02.009
10. Liu J, Li W, Zhu X, et al. Surfactin effectively inhibits Staphylococcus aureus adhesion and biofilm formation on surfaces. *Appl Microbiol Biotechnol*. 2019;103(11):4565–4574. doi:10.1007/s00253-019-09808-w
11. Chen X, Lu Y, Shan M, Zhao H, Lu Z, Lu Y. A mini-review: mechanism of antimicrobial action and application of surfactin. *World J Microbiol Biotechnol*. 2022;38(8):143. doi:10.1007/s11274-022-03323-3
12. E SS, Carvalho J, Aires CP, Nitschke M. Disruption of Staphylococcus aureus biofilms using rhamnolipid biosurfactants. *J Dairy Sci*. 2017;100(10):7864–7873. doi:10.3168/jds.2017-13012
13. Marangon CA, Martins V, Ling MH, et al. Combination of rhamnolipid and chitosan in nanoparticles boosts their antimicrobial efficacy. *ACS Appl Mater Interfaces*. 2020;12(5):5488–5499. doi:10.1021/acsami.9b19253
14. Kim LH, Jung Y, Yu HW, Chae KJ, Kim IS. Physicochemical interactions between rhamnolipids and pseudomonas aeruginosa biofilm layers. *Environ Sci Technol*. 2015;49(6):3718–3726. doi:10.1021/es505803c
15. Li P, Chen X, Shen Y, et al. Mucus penetration enhanced lipid polymer nanoparticles improve the eradication rate of Helicobacter pylori biofilm. *J Control Release*. 2019;300:52–63. doi:10.1016/j.jconrel.2019.02.039
16. Salek K, Euston SR, Janek T. Phase behaviour, functionality, and physicochemical characteristics of glycolipid surfactants of microbial origin. *Front Bioeng Biotechnol*. 2022;10:816613. doi:10.3389/fbioe.2022.816613
17. Juma A, Lemoine P, Simpson A, et al. Microscopic investigation of the combined use of antibiotics and biosurfactants on methicillin resistant Staphylococcus aureus. *Front Microbiol*. 2020;11:1477. doi:10.3389/fmicb.2020.01477
18. Muller F, Honzke S, Luthardt WO, et al. Rhamnolipids form drug-loaded nanoparticles for dermal drug delivery. *Eur J Pharm Biopharm*. 2017;116:31–37. doi:10.1016/j.ejpb.2016.12.013
19. Mitchell MJ, Billingsley MM, Haley RM, Wechsler ME, Peppas NA, Langer R. Engineering precision nanoparticles for drug delivery. *Nat Rev Drug Discov*. 2021;20(2):101–124. doi:10.1038/s41573-020-0090-8
20. Park H, Otte A, Park K. Evolution of drug delivery systems: from 1950 to 2020 and beyond. *J Control Release*. 2022;342:53–65. doi:10.1016/j.jconrel.2021.12.030
21. Lee K, Zhang L, Yi Y, Wang X, Yu Y. Rupture of lipid membranes induced by amphiphilic janus nanoparticles. *ACS Nano*. 2018;12(4):3646–3657. doi:10.1021/acsnano.8b00759
22. Pinto RM, Lopes-de-Campos D, Martins M, Van Dijck P, Nunes C, Reis S. Impact of nanosystems in Staphylococcus aureus biofilms treatment. *Fems Microbiol Rev*. 2019;43(6):622–641. doi:10.1093/femsre/fuz021
23. Pelgrift RY, Friedman AJ. Nanotechnology as a therapeutic tool to combat microbial resistance. *Adv Drug Deliv Rev*. 2013;65(13–14):1803–1815. doi:10.1016/j.addr.2013.07.011
24. Watanabe T. 共焦点レーザー走査顕微鏡による緑膿菌バイオフィルムの観察 [Observation of Pseudomonas aeruginosa biofilm with confocal laser scanning microscope]. *Kansenshogaku Zasshi*. 1995;69(1):114–122. Japanese. doi:10.11150/kansenshogakuzasshi1970.69.114
25. Patel V, Ray D, Bahadur A, Ma J, Aswal VK, Bahadur P. Pluronic((R))-bile salt mixed micelles. *Colloids Surf B Biointerfaces*. 2018;166:119–126.
26. Korsmeyer RW, Gurny R, Doelker E, Buri P, Peppas NA. Mechanisms of solute release from porous hydrophilic polymers. *Int J Pharmaceut*. 1983;15(1):25–35. doi:10.1016/0378-5173(83)90064-9
27. Varjani SJ, Upasani VN. Core Flood study for enhanced oil recovery through ex-situ bioaugmentation with thermo- and halo-tolerant rhamnolipid produced by Pseudomonas aeruginosa NCIM 5514. *Bioresour Technol*. 2016;220:175–182.
28. Lotfabad TB, Abassi H, Ahmadkhaniha R, et al. Structural characterization of a rhamnolipid-type biosurfactant produced by Pseudomonas aeruginosa MR01: enhancement of di-rhamnolipid proportion using gamma irradiation. *Colloids Surf B Biointerfaces*. 2010;81(2):397–405. doi:10.1016/j.colsurfb.2010.06.026
29. Rukavina Z, Segvic KM, Filipovic-Grcic J, Lovric J, Vanic Z. Azithromycin-loaded liposomes for enhanced topical treatment of methicillin-resistant Staphyloccocus aureus (MRSA) infections. *Int J Pharm*. 2018;553(1–2):109–119. doi:10.1016/j.ijpharm.2018.10.024
30. Tseng BS, Zhang W, Harrison JJ, et al. The extracellular matrix protects P seudomonas aeruginosa biofilms by limiting the penetration of tobramycin. *Environ Microbiol*. 2013;15(10):2865–2878. doi:10.1111/1462-2920.12155
31. Albayaty YN, Thomas N, Hasan S, Prestidge CA. Penetration of topically used antimicrobials through Staphylococcus aureus biofilms: a comparative study using different models. *J Drug Deliv Sci Tec*. 2018;48:429–436. doi:10.1016/j.jddst.2018.10.015
32. Fernandez-Hidalgo N, Almirante B. Antibiotic-lock therapy: a clinical viewpoint. *Expert Rev Anti Infect Ther*. 2014;12(1):117–129. doi:10.1586/14787210.2014.863148
33. Hall-Stoodley L, Costerton JW, Stoodley P. Bacterial biofilms: from the natural environment to infectious diseases. *Nat Rev Microbiol*. 2004;2(2):95–108. doi:10.1038/nrmicro821
34. Dusane DH, Dam S, Nancharaiah YV, Kumar AR, Zinjarde SS. Disruption of Yarrowia lipolytica biofilms by rhamnolipid biosurfactant. *Aquat. Biosyst*. 2012;8:17.
35. Guan R, Yuan X, Wu Z, et al. Functionality of surfactants in waste-activated sludge treatment: a review. *Sci Total Environ*. 2017;609:1433–1442. doi:10.1016/j.scitotenv.2017.07.189
36. More TT, Yadav JS, Yan S, Tyagi RD, Surampalli RY. Extracellular polymeric substances of bacteria and their potential environmental applications. *J Environ Manage*. 2014;144:1–25. doi:10.1016/j.jenvman.2014.05.010

37. Kim SG, Giri SS, Yun S, et al. Synergistic phage-surfactant combination clears IgE-promoted Staphylococcus aureus aggregation in vitro and enhances the effect in vivo. *Int J Antimicrob Agents*. 2020;56(1):105997. doi:10.1016/j.ijantimicag.2020.105997
38. Du M, Xu D, Trinh X, et al. EPS solubilization treatment by applying the biosurfactant rhamnolipid to reduce clogging in constructed wetlands. *Bioresour Technol*. 2016;218:833–841. doi:10.1016/j.biortech.2016.07.040
39. Bhattacharjee A, Nusca TD, Hochbaum AI. Rhamnolipids mediate an interspecies biofilm dispersal signaling pathway. *ACS Chem Biol*. 2016;11(11):3068–3076. doi:10.1021/acschembio.6b00750
40. Grande R, Puca V, Muraro R. Antibiotic resistance and bacterial biofilm. *Expert Opin Ther Pat*. 2020;30(12):897–900. doi:10.1080/13543776.2020.1830060
41. de Freitas FJ, Vieira EA, Nitschke M. The antibacterial activity of rhamnolipid biosurfactant is pH dependent. *Food Res Int*. 2019;116:737–744. doi:10.1016/j.foodres.2018.09.005
42. Rodrigues LR, Teixeira JA. Biomedical and therapeutic applications of biosurfactants. *Adv Exp Med Biol*. 2010;672:75–87.
43. Dewangan NK, Tran N, Wang-Reed J, Conrad JC. Bacterial aggregation assisted by anionic surfactant and calcium ions. *Soft Matter*. 2021;17(37):8474–8482. doi:10.1039/D1SM00479D